Chemistry & Biology
Article

Quantification of Real-Time *Salmonella* Effector Type III Secretion Kinetics Reveals Differential Secretion Rates for SopE2 and SptP

Schuyler B. VanEngelenburg[1] and Amy E. Palmer[1,*]
[1]Department of Chemistry and Biochemistry, University of Colorado, UCB 215, Boulder, CO 80309, USA
*Correspondence: amy.palmer@colorado.edu
DOI 10.1016/j.chembiol.2008.04.014

SUMMARY

Gram-negative pathogenic bacteria such as *Salmonella* utilize the type III secretion system to inject bacterial effector proteins into a host cell. Upon entry, these effectors bind mammalian cell proteins, hijack cellular signaling pathways, and redirect cellular function, thus enabling bacterial infection. In this study we use the FlAsH/tetracysteine labeling system to fluorescently tag specific effectors in *Salmonella* to observe real-time secretion of these proteins into a mammalian host cell. The tetracysteine tag is genomically incorporated, thus preserving endogenous control of bacterial effectors. We demonstrate that two effectors, SopE2 and SptP, exhibit different secretion kinetics, as well as different rates of degradation within the host cell. These proteins respectively activate and suppress GTPase Cdc42, suggesting that there is a temporal hierarchy for effector delivery and persistence within the cell that is directly related to effector function.

INTRODUCTION

Salmonella subspecies are intracellular bacterial pathogens and the etiological agents associated with food poisoning and typhoid fever. *Salmonella* have evolved a sophisticated macromolecular protein complex called the type III secretion system (TTSS) to translocate bacterial effector proteins into the host cytosol. These bacterial effector proteins then coordinate invasion by modulating eukaryotic host signaling pathways such as actin cytoskeleton dynamics, vesicular transport, and nuclear responses associated with inflammation (Hardt et al., 1998; Zhou and Galan, 2001). Effectors exhibit antagonistic and synergistic functions; for example, SopE2 and SptP activate and repress, respectively, GTPase Cdc42 (Fu and Galan, 1999; Stender et al., 2000), whereas SipA, SopB, and SopE act in concert to trigger actin polymerization at sites of bacterial invasion (Fu and Galan, 1999; Zhou et al., 1999, 2001). This carefully concerted action of the bacterial effector repertoire is critical for bacterial persistence within the host (Hapfelmeier et al., 2004; Zhou and Galan, 2001). These actions are likely to be regulated both spatially and temporally to preserve the hierarchy of events necessary for invasion. Work by Kubori and Galan (2003) has shown that SopE, an effector highly homologous to SopE2, is rapidly degraded upon host cell entry, leaving SptP to deactivate bacterial-mediated actin polymerization. However, no temporal regulatory mechanisms have been reported for effector protein delivery, perhaps because of the dearth of available tools to monitor the spatiotemporal nature of effector secretion.

Translocation of bacterial effector proteins into host cells has traditionally been investigated by western blotting or immunofluorescence (Abrahams et al., 2006; Kubori and Galan, 2003), which have limited temporal resolution, or by enzymatic assays (Schlumberger et al., 2005; Sory and Cornelis, 1994), which are indirect and have low spatial resolution. Direct labeling of effectors with bulky fluorescent proteins perturbs TTSS processes (Akeda and Galan, 2005), thus preventing fluorescent proteins from being used to monitor direct protein translocation. Schlumberger et al. (2005) developed the first assay to image accumulation of effector proteins within a host cell by recruitment of a fluorescently labeled chaperone within the host. This assay is effective at monitoring the appearance of effectors within the host; however, because the fluorescence signal relies both on effector accumulation and chaperone recruitment, the assay does not directly monitor the kinetics of secretion. The fluorescein-based biarsenical small molecule FlAsH offers a convenient alternative for direct labeling of tagged proteins within living cells. FlAsH was designed to bind a 12-amino-acid tetracysteine (TC) motif with high affinity and specificity (Adams et al., 2002; Martin et al., 2005). Previously, Enninga et al. (2005) demonstrated that the FlAsH/TC system can be used to fluorescently label effector proteins expressed on an exogenous plasmid. Here we extend this work and develop a system that is sufficiently sensitive to detect secretion of effectors under endogenous control. By monitoring disappearance of the labeled effector from the bacteria, we can directly measure the kinetics of secretion. Moreover, by incorporating the nonsecreted mCherry fluorescent protein as a bacterial marker we can normalize for Z-plane movement and detect accumulation of effectors in real time within mammalian cells.

In this work we focus on two *Salmonella* effectors, SptP and SopE2, because their demonstrated antagonistic activities make them likely candidates for effectors who are regulated temporally, either in their delivery or in their host cell-mediated degradation (Fu and Galan, 1999; Hardt et al., 1998). The FlAsH/TC labeling system was combined with live cell microscopy to monitor effector secretion throughout the invasion process. We identify an unprecedented difference in secretion rates between SopE2 and SptP, as well as a difference in the rate of host

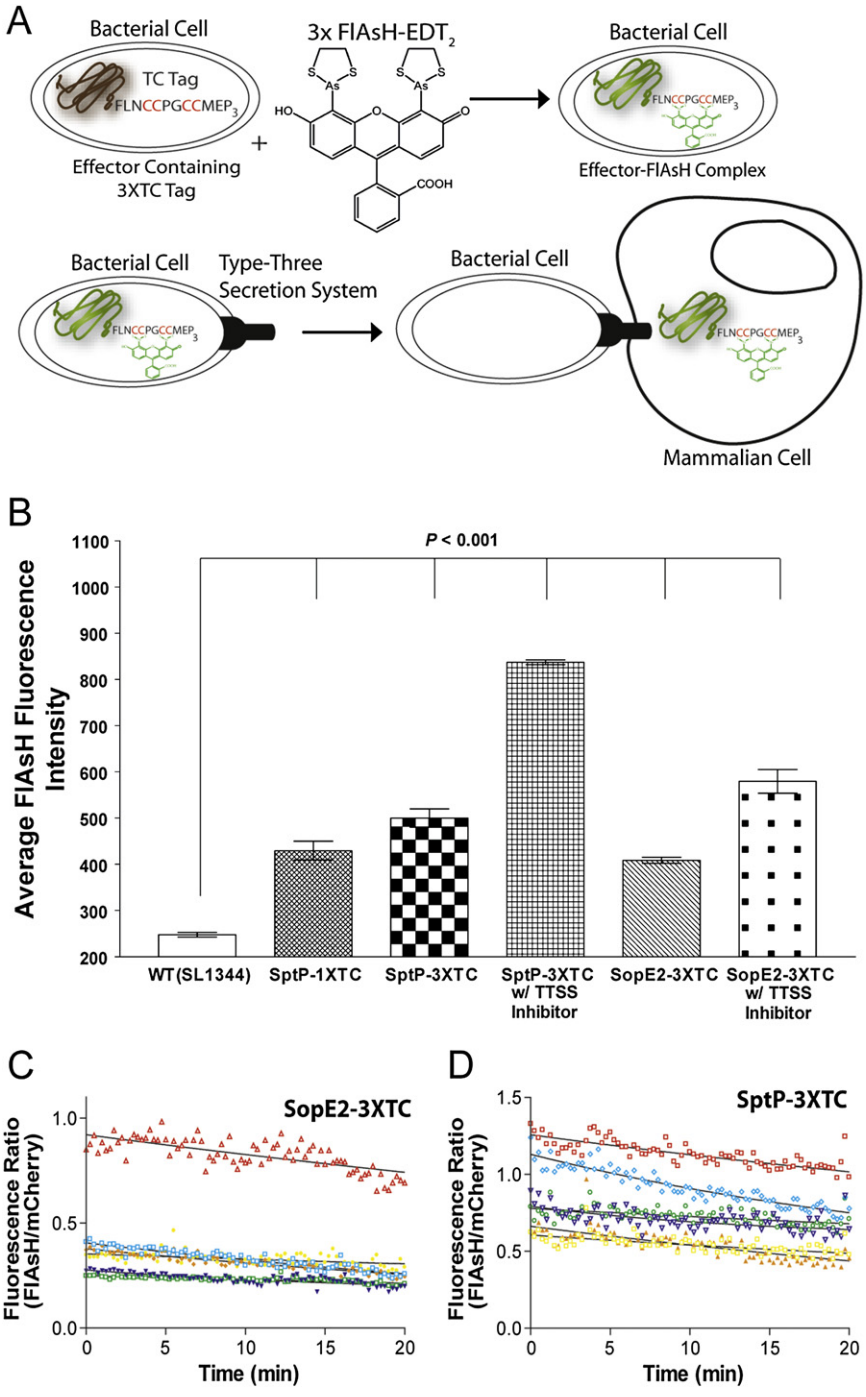

Figure 1. Visualizing Fluorescently Labeled Effectors in *Salmonella*

(A) Schematic illustration of the FlAsH labeling strategy for *Salmonella* strains expressing 3XTC effectors. (B) Average background-corrected FlAsH fluorescence intensity of different *Salmonella* strains. A significant increase ($p < 0.001$) in the average FlAsH signal intensity was observed for strains expressing TC-tagged effectors, with the 3XTC tag exhibiting a small but significant increase in intensity as compared with the 1XTC. Treating bacteria with the TTSS inhibitor **1** resulted in an increase in the FlAsH signal intensity for both SptP- and SopE2-3XTC. Error bars represent SEM ($n > 100$ individual bacteria were quantified for each group). Bacteria were selected and fluorescence was quantified as described in Experimental Procedures. Comparison of TTSS leak rates of individual bacteria in the absence of host cell contact for FlAsH labeled (C) SopE2-3XTC and (D) SptP-3XTC. The slow decay of FlAsH fluorescence in the absence of mammalian cell contact is a combination of the documented leak of effectors and FlAsH photobleaching. There is no significant difference ($p = 0.8526$) in the leak rate ($k_{leak/bleach}$) between the two labeled effector proteins ($n = 8$ for each). Statistical comparisons were made using a two-tailed t test with post-F test to confirm the assumption of equal variances ($p = 0.4649$). Data represent mean ± SEM.

cell-mediated degradation, which correlates with the known function of these effectors in manipulating Cdc42 signaling.

RESULTS

In situ fluorescence labeling of bacterial effectors and visualization of type III secretion by fluorescence microscopy is depicted in Figure 1A. To preserve endogenous control of TTSS effector expression, the TC tag was genomically incorporated into the *Salmonella* effector genes SptP and SopE2 using the λ Red recombinase system developed by Datsenko and Wanner (2000). As illustrated in Figure S1 (see the Supplemental Data available with this article online) the expression level of TC-tagged effectors is identical to nontagged effectors. Therefore, this strategy ensures that effector proteins are expressed at wild-type levels from their endogenous promoters, thus minimally perturbing the delicate balance of bacterial invasion. Because we anticipated low levels of protein expression, we compared FlAsH labeling of the single TC with a 3-fold repeat (3XTC; $[GSFLNCCPGCCMEP]_3$).

Salmonella strains encoding either SptP- or SopE2-3XTC were grown under invasion conditions and labeled with FlAsH. *Salmonella* expressing SptP- or SopE2-3XTC demonstrated a significant increase in FlAsH fluorescence intensity compared with wild-type (SL1344) bacteria (Figure 1B), indicating that FlAsH labeling is specific for bacteria expressing TC-tagged proteins. On average ~25% of bacteria were labeled with FlAsH, suggesting that only ~25% of bacteria express the effectors SopE2 and SptP when grown under invasion conditions. This is consistent with a previous report that only ~26% of bacteria express SipA, another invasion-associated effector, when grown under similar conditions (Schlumberger et al., 2005). We observe 20% higher FlAsH intensity for SptP compared with SopE2. Because the

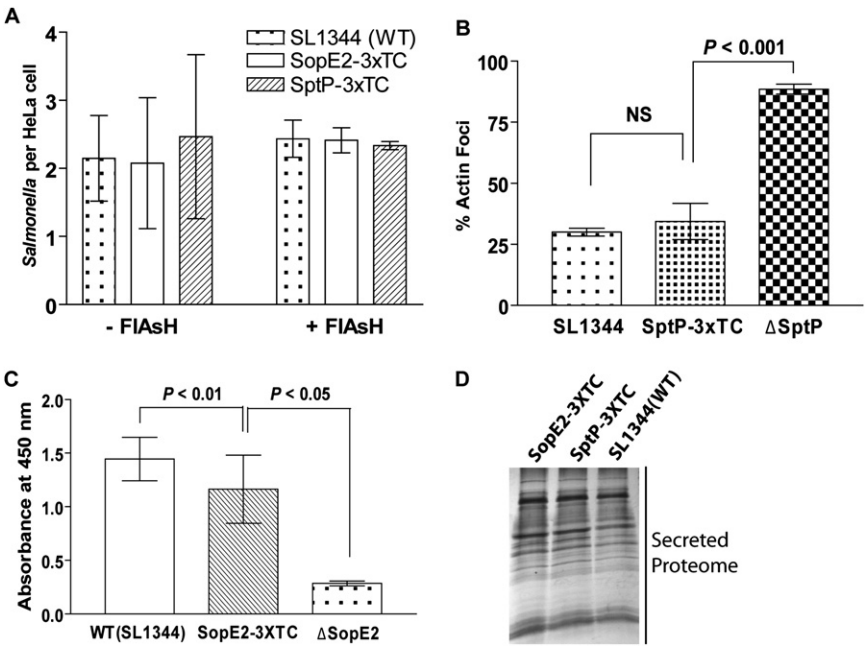

Figure 2. Incorporation of the 3XTC Tag onto the Effectors SopE2 and SptP Minimally Perturbs Invasiveness and Protein Function

(A) *Salmonella* strains in the presence and absence of the FlAsH and BAL were scored for the number of internalized bacteria per HeLa cell using DIC and fluorescence microscopy. No statistical difference between the number of *Salmonella* per HeLa cell for WT SL1344 and 3XTC epitope tagged strains ± FlAsH treatment was observed.

(B) Δ*sptp* resulted in a marked increase in actin-associated foci, whereas wild-type SL1344 and SptP-3XTC exhibited much lower levels, indicating membrane restoration in these strains. *Salmonella* strains expressing the mCherry bacterial marker were allowed to infect HeLa cells for 90 min and were then fixed. Cells were stained with phalloidin-FITC and Hoechst 33258 to visualize the host cell cytoskeleton and nuclei, respectively. For (A) and (B), $n \geq 40$ for each experiment; three independent experiments for a total $n > 120$.

(C) HeLa cells were infected with *Salmonella* strains; 5 hr after infection the growth medium was harvested and secreted IL-8 was quantified using an ELISA. Similar to wild-type SL1344, SopE2-3XTC induces the production of IL-8, although the extent of IL-8 production is slightly reduced ($p < 0.01$). Conversely, a bacterial strain carrying a null mutation in SopE2 (Δ*sope2*) is significantly attenuated for IL-8 production ($p < 0.05$ compared with SopE2-3XTC). Experiments were performed in triplicate. For (A–C) data represent mean ± SD.

(D) The secreted proteome (invasion-inducing conditions) was TCA precipitated from the culture supernatant and resolved using SDS-PAGE. No change in secreted protein levels is observed for the strains SptP- and SopE2-3xTC compared with wild-type.

fluorescence intensity of FlAsH can vary in different environments (Enninga et al., 2005; Martin et al., 2005), we determined the FlAsH labeling efficiency (defined as FlAsH intensity per protein) for SopE2 versus SptP. We observed a 2-fold increase in the FlAsH fluorescence/protein ratio for SopE2-3XTC compared with SptP-3XTC, indicating that labeling of SopE2 yields a higher fluorescence signal (Figure S2). Thus, the higher FlAsH signal for SptP versus SopE2-3XTC indicates that SptP is expressed at higher levels than SopE2. *Salmonella* strains expressing 3XTC-tagged SptP yielded small but significant increases in fluorescence intensity compared with SptP-1XTC, prompting us to use the 3XTC tag for all subsequent experiments. Given the marginal increase in FlAsH intensity (~15%), we suspect that fewer than three FlAsH molecules bind per 3XTC. We are currently comparing the fluorescence intensities for 1X, 2X, and 3X TC tags and optimizing the signal enhancement.

Treatment of bacteria with a recently identified small molecule (3,5-dichlorosalicylaldehyde benzoylhydrazone; **1**), which inhibits type III secretion of effectors (Hudson et al., 2007), resulted in an increase (~30%–40%) in FlAsH signal intensity over non-treated bacteria. The observed increase indicates that a subset of the labeled effector pool is lost prior to infection, consistent with reports that the *Salmonella* TTSS possesses a slow intrinsic leak when grown under TTSS-inducing conditions (Collazo et al., 1995; Schlumberger and Hardt, 2006). To characterize the kinetics of this leak, we labeled SptP and SopE2 with FlAsH and monitored the fluorescence decay in the absence of mammalian cells. A slow decrease in FlAsH fluorescence in the absence of host cell contact was observed ($k_{leak/bleach}$(SopE2-3XTC) = $3.2 \times 10^{-4} \pm 8.5 \times 10^{-5}$ s^{-1}, n = 8; $k_{leak/bleach}$(SptP-3XTC) = $3.0 \times 10^{-4} \pm 8.2 \times 10^{-5}$ s^{-1}, n = 8). This decrease is likely due to a combination of effector leakage and photobleaching (Figures 1C and 1D). There is no difference between the fluorescence decay of SptP and SopE2 ($p = 0.8526$).

To address whether addition of the 3XTC tag and/or treatment with FlAsH perturbed TTSS function and the coordinated action of effectors, we performed a quantitative bacterial invasiveness assay. We reasoned that if incorporation of the 3XTC tag onto effectors or treatment with FlAsH compromised either bacterial viability or the ability of bacteria to invade HeLa cells, we would see a reduction in the number of internalized bacteria. As depicted in Figure 2A, we detected no difference in the invasiveness of the SopE2-3XTC and SptP-3XTC strains when compared with wild-type SL1344, suggesting that incorporation of the tag did not significantly perturb TTSS function. Additionally, we detected no difference in invasiveness due to FlAsH and BAL treatment, and verified that FlAsH treatment did not perturb the overall viability of *Salmonella* using a growth assay (Figure S3).

We next addressed whether the activities of the effectors themselves were perturbed by incorporation of the 3XTC tag. SptP restores membrane architecture after internalization of invading bacteria and regulates the activity of Cdc42. To quantify SptP activity, internalized bacterial microcolonies were scored for their association with actin rich foci (Figure 2B). As expected, a bacterial strain deficient in SptP (*Δsptp*) showed strong enrichment of actin, whereas the WT strain SL1344 showed a drastic reduction in actin association with microcolonies due to restoration of membrane architecture. We observed a comparable

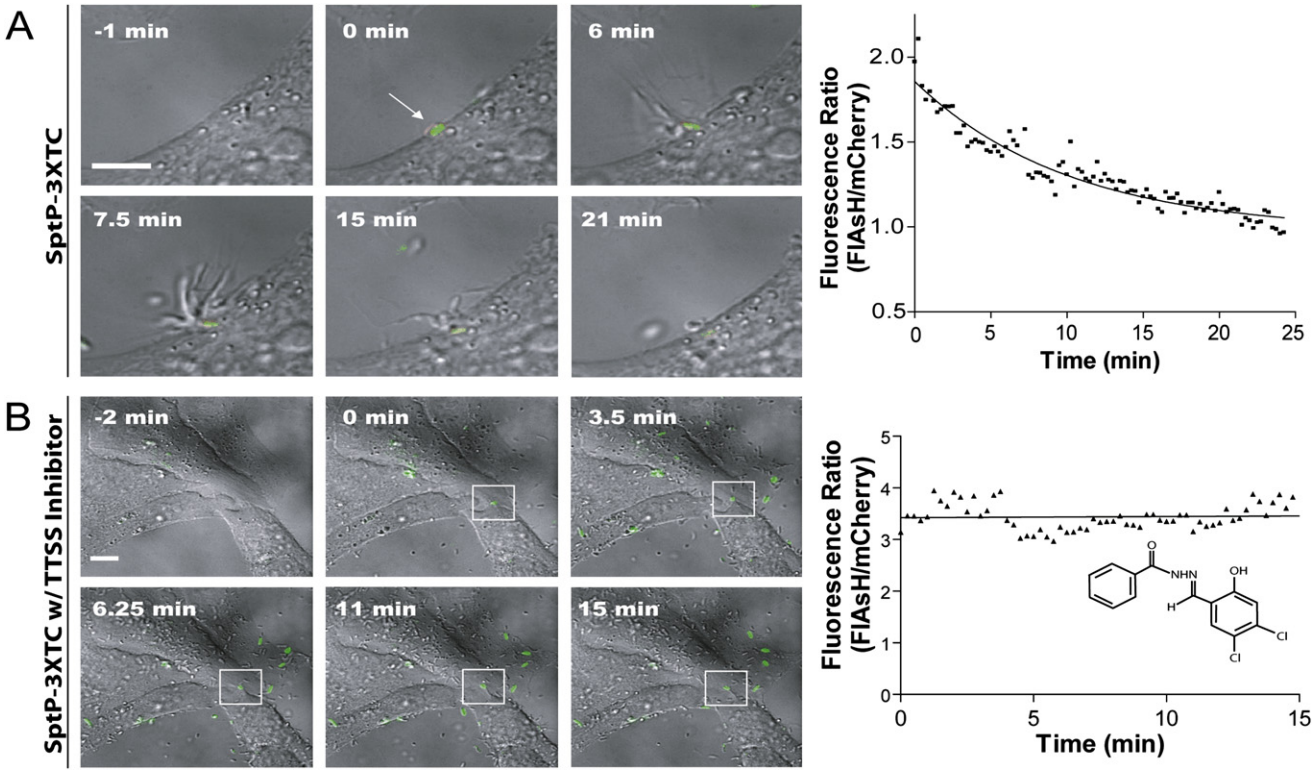

Figure 3. Representative Time Course for Invasion of HeLa Cells by Individual Bacteria

(A) Images of FlAsH labeled SptP-3XTC *Salmonella* infecting a HeLa cell. Presented are overlaid images of the FlAsH channel (in green) and DIC channel. For clarity, the mCherry fluorescence channel is not depicted. *Salmonella* triggers membrane ruffling (6 min and 7.5 min), bacterial internalization (7.5 min and 15 min), and restoration of the membrane architecture (21 min). The mCherry fluorescence channel was used to normalize for Z-plane movement during bacterial internalization. A decrease in the intrabacterial FlAsH fluorescence is observed over the course of invasion.

(B) Representative HeLa infection using SptP-3XTC *Salmonella* pretreated (3 hr) with the TTSS inhibitor **1**. The box highlights quantified *Salmonella* in contact with a HeLa cell over a relevant infection period. No TTSS-mediated membrane ruffling events, actin foci, or (FlAsH/mCherry) decreases were observed. Scale bar represents 10 μm.

reduction in the number of bacterially associated actin foci in the SptP-3XTC strain compared with wild-type SL1344, indicating SptP function is not compromised by addition of the 3XTC tag. SopE2 activates Cdc42, which induces a proinflammatory response leading to the production of interleukin-8 (IL-8) (Huang et al., 2004; Patel et al., 2005). To assess SopE2 activity, we measured the production of IL-8 using an enzyme-linked immunosorbent assay (ELISA). As depicted in Figure 2C, *Δsope2* showed a marked reduction in IL-8 production as compared with the wild-type SL1344 strain. The SopE2-3XTC strain elicited a significant proinflammatory response, although there was a slight reduction compared with wild-type SL1344. Collectively, these results suggest that the 3XTC tag and FlAsH labeling of the SopE2 and SptP effectors minimally perturbs effector function and the TTSS-mediated invasion process. No significant perturbations in the levels of other effector proteins secreted by the TTSS in SptP- and SopE2-3XTC-tagged strains compared to wild-type bacteria were observed (Figure 2D).

Having established that 3XTC-tagged effectors expressed under endogenous control result in detectable FlAsH labeling, and that effector function is not significantly perturbed by this labeling technology, we then assessed whether we could monitor translocation of FlAsH labeled effector proteins into HeLa epithelial cells. Initially, we observed large focal plane deviations due to bacterial cell engulfment. To circumvent this problem and enable the use of wide-field fluorescence microscopy for monitoring type III secretion processes, we engineered *Salmonella* strains to express a nonsecreted fluorescent protein, mCherry (Shaner et al., 2004). This method yields a ratiometric readout (FlAsH/mCherry), where decreases in the ratio correspond with disappearance of the FlAsH signal (i.e., secretion) regardless of the focal position of bacteria. We observed heterogeneity in the initial FlAsH/mCherry fluorescence ratios due to small differences in FlAsH labeling and mCherry expression between the two strains used in this study (Figure S4A). Although we observe some heterogeneity in the initial fluorescence ratios between the two effectors, the secretion rate constant does not depend on the starting ratio or ratiometric span of individual invading bacteria (see Figures S5A–S5F). A representative time-lapse experiment of FlAsH labeled SptP-3XTC is presented in Figure 3 and Movie S1. Over the course of 15–20 min we observed the hallmark invasion phenotype of membrane ruffling, bacterial engulfment, and membrane architecture restoration. This latter phenotype results from the action of SptP, demonstrating that fusion of the 3XTC motif to SptP does not inhibit its function (Fu and Galan, 1999). As seen in Figure 3A, upon mammalian

cell contact the ratio of FlAsH/mCherry fluorescence decreases over time due to secretion of SptP into the host cell. Analogously, SopE2 secretion was readily detected upon mammalian cell contact (Figure S6A).

Treatment of SptP-3XTC with TTSS inhibitor **1** prevented cellular invasion and mammalian cell contact-mediated decreases in fluorescence, as illustrated in Figure 3B. For *Salmonella* treated with inhibitor **1** we did not detect any membrane ruffling events during the course of an invasion, indicating that invasion-associated effector proteins were not released. Likewise, treatment of SopE2-3XTC with inhibitor **1** abolished contact-mediated decreases in fluorescence (Figure S6B). As a control we measured the rate of decay for FlAsH-treated wild-type SL1344 bacteria. These bacteria do not contain a tetracysteine tag, but on average do exhibit a small amount of nonspecific staining (Figure 1B). As demonstrated in Figure S7, there is a slow decay in fluorescence over time. This decay appears more linear than exponential, but we fit the data to a single exponential to compare the rate constants. The average rate of decay was $6.2 \pm 3.4 \times 10^{-4}$ s^{-1} for internalized bacteria and $5.4 \pm 8.8 \times 10^{-4}$ s^{-1} for bacteria in the absence of mammalian cell contact. These decay rates are comparable to the leak/bleach rate for fluorescence decay of nonsecreted effectors ($\sim 3.0 \times 10^{-4}$ s^{-1}) (Figures 1C and 1D), suggesting that photobleaching dominates this process.

We chose to examine SptP and SopE2 because their demonstrated antagonistic activities make them likely candidates for effectors that are regulated temporally, either in their delivery or degradation (Fu and Galan, 1999; Hardt et al., 1998). The secretion kinetics of representative individual bacteria are presented in Figure 4, demonstrating that SopE2 is secreted faster than SptP. The fit parameters for all quantified bacteria are presented in Figure S5E. Type III secretion was modeled as an irreversible first-order decay process as effectors are translocated in an ATP-dependent manner (Akeda and Galan, 2005). Quantification revealed that SopE2-3XTC was secreted into HeLa (epithelial) cells at a rate roughly 2-fold that of SptP-3XTC ($k_{secretion(SopE2)} = 4.0 \times 10^{-3} \pm 0.4 \times 10^{-3}$ s^{-1} versus $k_{secretion(SptP)} = 2.1 \times 10^{-3} \pm 0.4 \times 10^{-3}$ s^{-1}) (Figure 4B). Bacteria that did not contact mammalian cells displayed only minimal changes in the FlAsH/mCherry ratio over the duration of the experiment. The average rate of fluorescence decay for bacteria not contacting mammalian cells was $1.4 \times 10^{-4} \pm 8.6 \times 10^{-5}$ s^{-1}, and was the same for SptP-3XTC and SopE2-3XTC. These rates are consistent with the rate we observed for the combination of photobleaching and the slow effector leak in the absence of mammalian cells (Figures 1C and 1D).

To further show that the secretion rates we observed are not due to the cell type used, we chose to quantify secretion of the effectors SopE2 and SptP in a marcrophage-like cell line. The secretion rates in RAW 264.7 macrophage-like cells were comparable to those in HeLa cells, with SopE2-3XTC yielding an average secretion rate of $4.5 \times 10^{-3} \pm 8.8 \times 10^{-4}$ s^{-1} (n = 4), and SptP-3XTC yielding an average secretion rate of $2.2 \times 10^{-3} \pm 4.8 \times 10^{-4}$ s^{-1} (n = 4) (Figures 5A and 5B). To ensure that contact-dependent decreases in fluorescence were not due to interaction with membrane ruffles or bacterial internalization, TTSS inhibitor **1**-treated bacteria were opsonized and phagocytosed by RAW 264.7 macrophage-like cells. Inhibitor-treated bacteria internalized by macrophage in a TTSS-independent manner

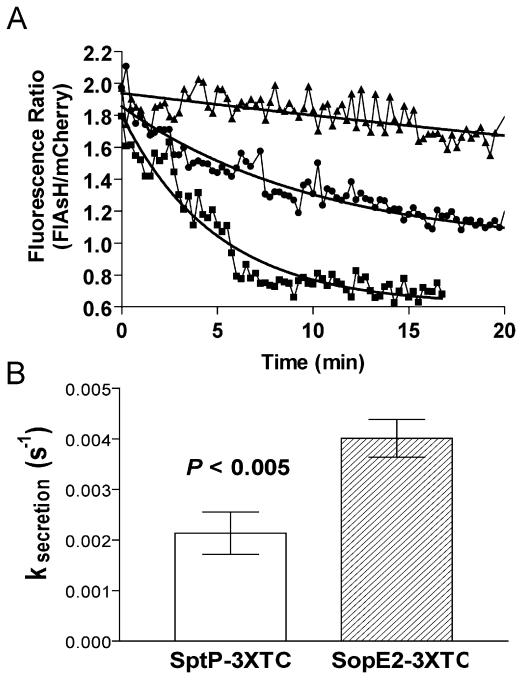

Figure 4. *Salmonella* Effector SopE2 Is Secreted Faster Than Effector SptP

(A) Representative kinetic traces and corresponding fits for SopE2 (circles, $R^2 = 0.9196$), SptP (squares, $R^2 = 0.9169$), and a control bacterium expressing FlAsH labeled SptP but which did not contact HeLa cells during the invasion (triangles, $R^2 = 0.5143$). Figure S5 presents the fitting parameters for the remainder of the bacteria.

(B) Average first-order rate constants for SptP-3XTC ($k_{secretion} = 2.1 \times 10^{-3} \pm 0.4 \times 10^{-3}$ s^{-1}; SEM, n = 11) and SopE2-3XTC ($k_{secretion} = 4.0 \times 10^{-3} \pm 0.4 \times 10^{-3}$ s^{-1}; SEM, n = 14). SopE2-3XTC shows a significant increase in the rate of type III secretion compared with SptP-3XTC ($\alpha = 0.05$; p = 0.0029). Data represent mean ± SEM.

exhibited fluorescence decays similar to those observed for bleach/leak kinetics ($k_{bleach(SopE2)} = 4.6 \times 10^{-4} \pm 1.5 \times 10^{-4}$ s^{-1} [n = 3] and $k_{bleach(SptP)} = 2.4 \times 10^{-4} \pm 3.7 \times 10^{-4}$ s^{-1} [n = 3]) (Figures 5C and 5D). This control demonstrates that the fluorescence decay for SopE2-3XTC and SptP-3XTC represent specific secretion through the TTSS. Furthermore, because this decay rate is similar to that observed for the bleach/leak rate of decay for bacteria not contacting mammalian cells, we conclude that the rate of photobleaching dominates that of effector leakage. These results provide direct evidence that temporal regulation of effectors can occur by modulating the kinetics of effector delivery, and suggest that delivery of antagonistic effectors may be preorganized to ensure that activators are secreted more rapidly than repressors. We observed invasion initiation throughout a time course experiment, highlighting the importance of monitoring secretion at the single bacterium level, as bulk assays average the kinetics of multiple invasions that occur at different times.

To build a complete picture of the regulation of SopE2 versus SptP, we examined the rate of degradation within the host cell. Previously, Kubori and Galan (2003) demonstrated that the antagonistic SopE and SptP activities are regulated through differential proteasomal degradation rates, with SopE being turned over at a $\sim$6.5× elevated rate ($t_{1/2} \approx 7.5$ min versus 45

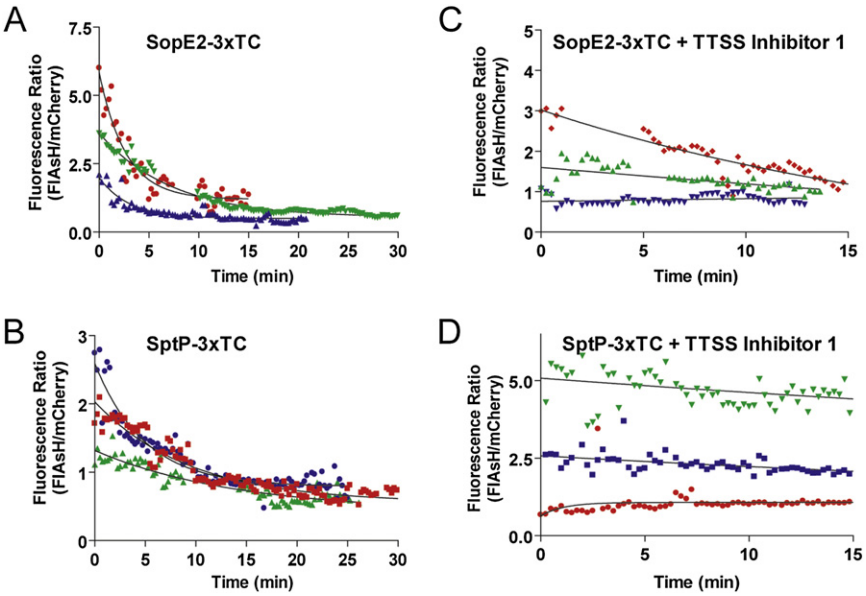

Figure 5. Quantification of SopE2- and SptP-3xTC Secretion with Mouse Macrophage-like (RAW 264.7) Cells

FlAsH-labeled effector strains (A) SopE2-3xTC and (B) SptP-3XTC were quantified for effector secretion after infecting RAW264.7 cells. (C) SopE2-3XTC and (D) SptP-3XTC strains were pretreated with TTSS inhibitor (**1**) prior to FlAsH staining and opsonization. RAW 264.7 cells were allowed to phagocytose opsonized *Salmonella* strains and individual bacteria were quantified using the FlAsH/mCherry fluorescence ratio.

min) (Kubori and Galan, 2003). Using the method of Kubori and Galan (2003), we quantified translocated effector proteins by western blotting. As shown in Figure 6A, SopE2-3XFLAG was degraded with a $t_{1/2}$ = 40 min, as compared with SptP-3XFLAG $t_{1/2}$ = 110 min, yielding a ~2.8× difference in mammalian cell-mediated degradation kinetics. We also observed similar degradation rates by inhibiting de novo effector protein synthesis postinvasion, indicating that the persistence of the effectors SptP- and SopE2-3XFLAG is not the result of resynthesis after bacterial internalization (Figure 6B). The observed 2.5× difference in $t_{1/2}$ of SptP (Kubori's 2003 study versus this work) may result from the different cell types used in the respective experiments or the addition of the 3XFLAG epitope to the effectors. Even so, it is clear that SopE2 is degraded faster than SptP and that the relative difference in rates (SopE2 versus SptP) is less than that observed for SopE versus SptP. Therefore, in addition to enhanced secretion rates, SopE2 is also degraded ~2.8× faster than the repressor SptP.

DISCUSSION

To coordinate invasion, *Salmonella* need to turn on and turn off mammalian cell signaling pathways at explicit times.

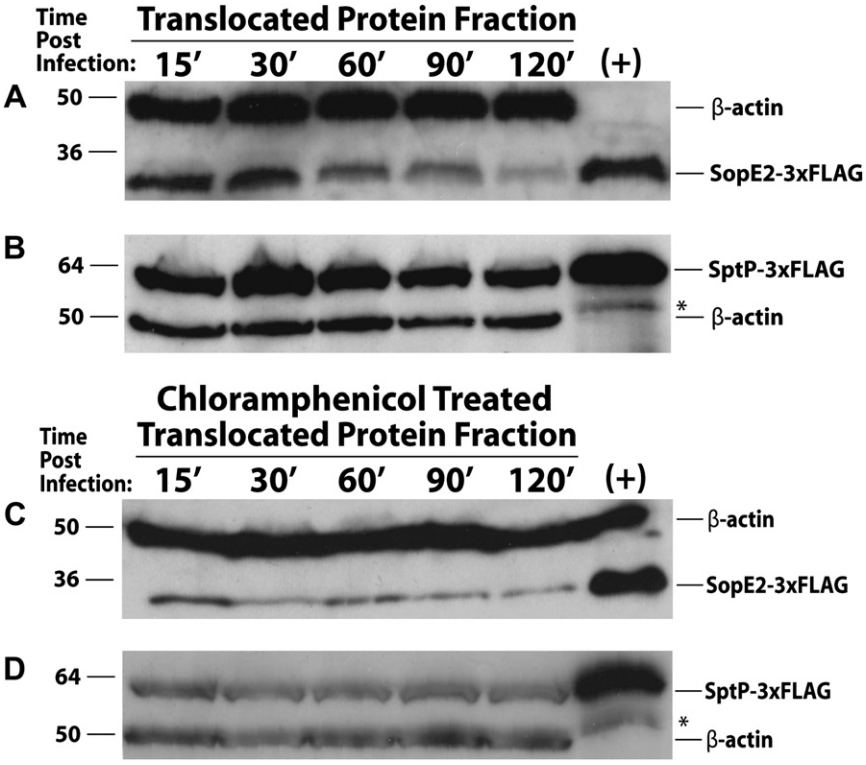

Figure 6. Intracellular Degradation Time Course for Translocated SopE2- and SptP-3XFLAG Effectors

(A) SopE2-3XFLAG SL1344 infection time course illustrating gradual degradation kinetics.
(B) SptP-3XFLAG SL1344 infection time course.
(C) SopE2-3XFLAG SL1344 infection time course showing similar degradation rates with inhibition of de novo protein synthesis using chloramphenicol.
(D) SptP-3XFLAG SL1344 infection time course performed in the presence of chloramphenicol. Intact bacteria were separated by selective lysis of mammalian cells to ensure selective measurement of translocated effector protein. SopE2 and SptP are both present in host cells postinvasion (~15 min). The degradation rate for SopE2-3XFLAG is approximately 2.8× that of SptP-3XFLAG. Anti-β-actin antibody was used as loading control. Positive control lane (+) represents 20% of input *Salmonella* for each time course (total bacterial lysate). Asterisk denotes anti-FLAG M2 crossreactive bacterial lysate protein in positive control lane.

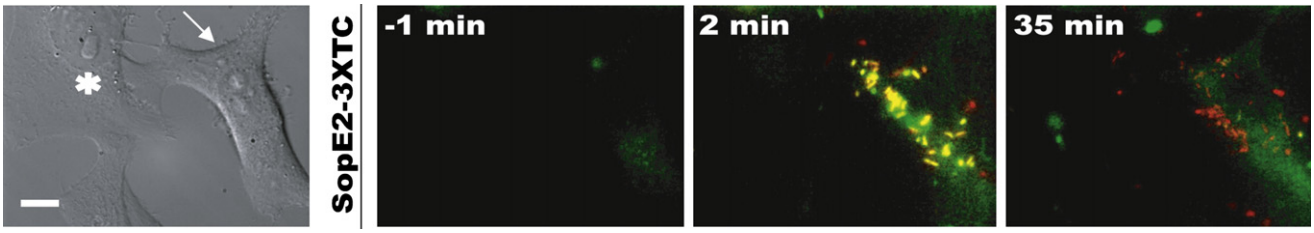

Figure 7. Real-Time Accumulation of SopE2-3XTC/FlAsH Fluorescence in a Mammalian Cell

Presented are overlaid images of the mCherry channel (red) and FlAsH channel (green), where yellow denotes direct overlap between the two channels. At −1 min there is little cellular fluorescence in either channel. At 1 min postinvasion, bacteria are clearly yellow/green, indicating the presence of SopE2. At 35 min postinvasion, the bacteria are red because they have secreted all their SopE2 but retain the mCherry bacterial marker. Conversely, at 35 min the mammalian cell fluorescence in the FlAsH channel increases due to accumulated effector protein. An increase in mammalian cell fluorescence occurs only for the cell that is readily invaded (arrow) with no signal occurring in the cells that were not invaded (*). Scale bar represents 10 μm.

Consequently, *Salmonella* have evolved a repertoire of effector proteins, some of which act in concert and some of which act in direct opposition to one another. To maintain the hierarchy of events necessary for invasion, these effectors must be regulated both spatially and temporally. In this work, we demonstrate that two effectors exhibiting antagonistic functions are secreted at different rates. The difference in temporal regulation of SopE2 versus SptP and SopE versus SptP correlates well with their relative known functions. SopE2 possesses guanine nucleotide exchange factor (GEF) activity toward Cdc42 (Stender et al., 2000), where Cdc42 activation leads to a nuclear proinflammatory response (Patel et al., 2005). In contrast, SopE activates Rac1, contributing to actin polymerization events during bacterial invasion (Patel et al., 2005; Rudolph et al., 1999). Postinvasion, SptP serves to deactivate Cdc42 and Rac1, leading to repression of nuclear responses and membrane architecture restoration, respectively (Fu and Galan, 1999). The enhanced rate of secretion of SopE2 would enable activation of Cdc42 before SptP is delivered. Although Kubori and Galan (2003) did not detect differential secretion of SopE and SptP, this may result from the limited temporal resolution of their assay. Upon bacterial invasion, the entire pool of SopE is degraded within 15 min, which corresponds with the time required for invasion. Conversely, SopE2 persists within the host cell (≥120 min) far longer than SopE, perhaps to provide a more graded nuclear response.

In the present work, we modified an experimental approach employed previously by Enninga et al. (2005) and made three improvements. First, we demonstrate that the TC tag can be genomically incorporated, thus allowing us to study effectors expressed under control of their endogenous promoter. This is important as it ensures that the system is minimally perturbed. Second, we discovered that the 3XTC allows for higher fluorescent labeling than the 1XTC. We believe that the current 3XTC tag is not fully optimized; we are therefore in the process of optimizing this tag to enhance the fluorescence signal, using a strategy similar to that reported for enhancing 1XTC sensitivity (Martin et al., 2005). Last, by incorporating the mCherry fluorescent protein as a nonsecreted bacterial marker, we were able to monitor secretion on a standard wide-field fluorescent microscope. The mCherry bacterial marker enables us to identify accumulated effectors within the host cell, paving the way for studying real-time effector localization and trafficking. As depicted in Figure 7, the decrease in bacterial FlAsH fluorescence correlates with an increase in mammalian fluorescence, where the bacteria are readily marked by the presence of mCherry. Our current signal:noise is low, requiring high MOIs to observe effector accumulation; however, we are hopeful that this signal can be increased upon optimization of the 3XTC. Based on our findings, we believe this experimental approach shows promise for monitoring the kinetics of labeled effector trafficking and localization within living host cells in real time.

The FlAsH/TC system displays a number of advantages over other approaches to studying type III secretion. The primary methods for monitoring effector secretion are western blotting and immunofluoresence. Though these methods can provide critical snapshots of effector concentration and localization, the first time point is typically acquired at 15 min. As is evident from Figure 4, the effector protein from an individual bacterium is >75% depleted at this 15 min time point. Therefore, western blotting and immunofluorescence techniques are incapable of resolving fast secretion events. Additionally, we found that bacteria initiate invasion throughout the time course, highlighting the importance of monitoring secretion from individual bacteria. Therefore, bulk assays assessing effector translocation, such as western blotting, temporally average multiple bacterial invasions. Schlumberger et al. (2005) developed an innovative assay to monitor accumulation of effector proteins within a host cell by recruitment of a fluorescently labeled chaperone expressed within the host cell. Though this assay is effective at monitoring localization of effector proteins, it does not permit direct assessment of effector secretion kinetics. Perhaps for this reason, the kinetics of recruitment upon SipA accumulation was found to be heterogeneous. Moreover, this method is limited to studying effectors for which the chaperone has been identified. Tetracysteine tagging and FlAsH labeling of endogenously expressed effectors enables us to single out a specific effector without perturbing the remaining effectors and provides a system for monitoring effector translocation into live mammalian cells.

SIGNIFICANCE

We have demonstrated a powerful technique for quantitatively assaying type III secretion kinetics of endogenous *Salmonella* effector proteins. Because of the time resolution of this method, we were able to discern a difference in the rate at which effectors are delivered into the host. We propose

that the combined effect of faster secretion and faster degradation for SopE2 compared with SptP creates a temporal hierarchy based on effector function. This study highlights the power of using real-time methods to study type III secretion processes. As pathogens are hard-pressed to rapidly establish a replicative niche within the host, more sophisticated spatiotemporal regulatory mechanisms will undoubtedly be uncovered as our understanding of host pathogen interactions matures.

EXPERIMENTAL PROCEDURES

Media and Reagents

Oligonucleotides were obtained from IDT (Coralville, IA). Polymerase chain reaction (PCR) amplifications of the TC tag and resistance cassette DNA was carried out using Phusion DNA polymerase (Finnzymes; New England Biolabs, Ipswich, MA) to ensure the fidelity of chromosomal insertions. *Taq* DNA polymerase was used for all colony PCR reactions to ensure the presence of the TC tag-tagged genes. L-arabinose (Sigma, St. Louis, MO) was used at a concentration of 50 mM for induction of bacterial cultures. LB was purchased from Invitrogen (Carlsbad, CA). SOB media was prepared as described (Hanahan, 1983).

Plasmids

Plasmids pKD46, pKD3, pKD4 were obtained from B. Wanner (Purdue University, West Lafayette, IN) by means of C. Detweiler (University of Colorado, Boulder, CO). Plasmid pKD46 carries the bacteriophage λ Red genes (γ, β, and *exo*), which catalyze chromosomal recombination using double-stranded linear DNA in bacteria (Datsenko and Wanner, 2000). The plasmid pKD4 is a π-dependent suicide vector carrying the kanamycin-resistance gene (Kn^R) (Datsenko and Wanner, 2000).

Construction of the Template Plasmids pTetCys, p3XTetCys, and p3XFLAG

Oligonucleotide primers encoding the high-affinity tetracysteine coding sequence (GSFLNCCPGCCMEP) (Martin et al., 2005) and attB recombination sequences were used for amplification of the Kn^R resistance gene from plasmid pKD4. The resultant amplicon was cloned into the vector pDONR221 by recombination using the Gateway system (Invitrogen), yielding the vector pTetCys. Oligonucleotide primers encoding a 2× tetracysteine coding sequence, and attB sites were used to amplify a 3× tetracysteine-encoding amplicon from the vector pTetCys. This amplicon was recombined into the pDONR221 vector using the Gateway system (Invitrogen). The resulting vector p3XTetCys encodes the three copies of the tetracysteine epitope followed by the Kn^r resistance gene. The vector p3XFLAG was created using an identical procedure.

Construction of Plasmid pAMCh

The bacterial marker plasmid pAMCh was constructed from the parent plasmid pACYC177 (New England Biolabs). Oligonucleotide primers complementary to the fluorescent protein mCherry were used as primers for PCR amplification from the parent vector pRSET-B mCherry courtesy of R.Y. Tsien. The resulting amplicon was cloned into the pACYC177 vector using XhoI and HindIII restriction sites. The ribosomal protein promoter P-rpsM was cloned from the *Salmonella enterica* serovar LT2 genome using complementary oligonucleotides. The P-rpsM amplicon was cloned upstream of the mCherry coding sequence using the XhoI restriction site, yielding a vector capable of constitutive mCherry fluorescent protein expression.

Bacteria

Salmonella enterica serovar Typhimurium derived from the strain LT2, which harbors the plasmid pKD46, was used for all recombination exchanges described (λ Red). Strain SL1290 was used for creation of P22 bacteriophage stocks. The *Salmonella typhimurium* wild-type strain SL1344 (Str^R) was used for P22 transduction of the antibiotic resistance gene and the coupled epitope fusion. Where indicated, strains carrying null mutations in the TTSS effectors SopE2 and SptP were created using recombination exchanges with the kanamycin resistance gene as previously described (Datsenko and Wanner, 2000). *Eschericia coli* strains DH5α were used for all cloning experiments (Invitrogen).

FlAsH Fluorescence Intensity Quantification

Average fluorescent intensity analysis was performed on individual *Salmonella* (Figure 1B). Bacteria were stained with FlAsH (5 μM), washed three times with 0.25 mM BAL (1,2-dimercaptoethanol; Sigma) in Hank's Balanced Salt Solution (HBSS), and tethered to imaging dishes using poly(L)-lysine (100 μg × ml^{-1}) (Sigma). Random fields of view were chosen and images were acquired for the FlAsH and mCherry channels. These image files were then imported into ImageJ, background subtracted, and thresholded to the average intensity of background staining (WT SL1344, no TC tag); regions of interest (ROI) were autoassigned using the software ImageJ (NIH). These ROIs were then used as a masking template for the original background-subtracted image (no thresholding), and the average fluorescence intensity for each ROI was acquired. Greater than 100 individual bacteria ($n > 100$) were quantified from each group.

Invasiveness Assay

Invasion efficiency was quantified as previously described (Drecktrah et al., 2006). HeLa cells were seeded at a density of 3.0×10^5 cells per 3.5 cm^2 dish 18 hr prior to infection. *Salmonella* cultures were grown under invasion-associated TTSS-inducing conditions (0.3 M NaCl, low O_2, LB medium), and HeLa cells were infected with a multiplicity of infection (MOI) of 50. The infection was allowed to proceed for 15 min before the addition of 100 μg × ml^{-1} gentamycin (Sigma) to kill extracellular bacteria. The infection was allowed to proceed for an additional 75 min. The invasion process was quenched by the addition of 4% formaldehyde. Cells were then stained with 2 μg × ml^{-1} Hoechst 33258 dye for 20 min to visualize mammalian nuclei. This protocol allowed for visualization and differentiation of extracellular bacteria while leaving intracellular bacteria unlabeled. All strains of *Salmonella* used in these experiments express the fluorescent protein mCherry to mark individual bacteria for enumeration. Invasion efficiency was scored by DIC and fluorescence microscopy blind to the *Salmonella* strain under investigation. Random viewing fields were selected for enumerating the number of bacteria infecting each HeLa cell. Experiments for each genotype were performed in triplicate ($n \geq 40$ HeLa cells for each replicate). Where indicated, *Salmonella* strains were treated with 5 μM FlAsH-EDT_2 for 1 hr at 37°C and washed three times with 0.25 mM BAL in HBSS prior to infection.

SptP Activity Assay

The actin foci/membrane ruffling assay was performed as described previously (Kubori and Galan, 2003). HeLa cells were plated and infected with *Salmonella* as described previously. Infections were quenched as described. Cells were permeabilized with 0.1% Triton X-100 (Sigma) and stained with Hoechst 33258 and phalloidin-FITC (Sigma) to visualize nuclei and actin respectively. Experiments were performed using fluorescence microscopy blind to the *Salmonella* strain under investigation. Random fields of infected HeLa cells were scored for the association of bacterial microcolonies with actin-rich foci. All experiments were performed in triplicate ($n \geq 40$ bacterial microcolonies for each replicate).

SopE2 Activity Assay

Quantification of SopE2-mediated upregulation of interleukin-8 (IL-8) was performed as described (Huang et al., 2004). *Salmonella* cultures were grown under SPI-1 conditions as described. HeLa cells were seeded at a density of 4.0×10^4 cells per well in standard six-well plates 48 hr prior to infection (2% FCS DMEM medium). TTSS-induced bacteria were added at an MOI of 50. Infections were allowed to proceed for 1 hr before the addition of 100 μg × ml^{-1} gentamycin. Six hours postinfection the culture medium was collected and clarified by centrifugation at 14 krpm for 5 min. Quantification of IL-8 production was performed using an enzyme-linked immunosorbent assay according to the manufacturer's instructions (BioLegend, San Diego, CA). ELISA reactions were performed in triplicate for each genotype.

TCA Precipitation of the Secreted Proteome

Salmonella strains were grown overnight under invasion-associated conditions to induce SPI-1 effector secretion into the culture supernatants. Culture

supernatants were collected by centrifugation at 14 k × g for 30 min followed by 0.22 μm filtration. The supernatants were then precipitated with 10% TCA as described previously. Precipitated proteins were washed in acetone and redissolved in SDS-loading buffer and resolved using 10%–20% SDS-PAGE. Secreted proteins were visualized with Coomassie Brilliant Blue R-250 (Sigma).

Time-Lapse Microscopy

Fluorescence imaging of bacterial effector secretion was performed using an Axiovert 200M wide-field microscope (Zeiss, Thornwood, NY), equipped with Lambda 10-3 filter changer (Sutter Instruments, Navato, CA). This system is configured to allow rapid acquisition of fluorescence images to facilitate live-cell imaging. Images were acquired using METAFLUOR software (Universal Imaging, Sunnyvale, CA) and a Cascade 512B CCD camera (Roper Scientific, Trenton, NJ) with an EM Gain of 2500 and a 5 MHz transfer speed. All images were obtained using a 1.4 NA 100 × PlanAPO objective (Zeiss), and the following filter combinations: FlAsH: 495/10 (excitation), 542/50 (emission), 515 (dichroic filter cube); mCherry: 577/20 (excitation), 630/60 (emission), 595 (dichroic filter cube).

Kinetic Secretion Assay

SL1344 strains carrying 3XTC fusions to the effector proteins SopE2 and SptP were grown for ~16 hr at 37°C under invasion-associated conditions (LB 0.3M NaCl, low O_2, OD_{600} ~0.4–0.5) (Collazo and Galan, 1996). HeLa cells were seeded onto 3.5 cm^2 imaging dishes at ~70%–90% confluence. Macrophage-like RAW264.7 cell infections were treated identically to HeLa infections. Approximately 500 μl of bacterial culture was treated with 5 μM FlAsH-EDT_2 (Invitrogen) for 1 hr at 37°C before incubation (~10 min) with 10 μg × ml^{-1} poly(L)-lysine. Bacteria were then washed three times with Hank's HEPES Balanced Salt Solution (HHBSS) containing 0.25 mM BAL (2,3-dimercaptoethanol). HeLa cells were infected at an MOI of ~10 at 25°C. Image acquisition was initiated before infection, and frames for each channel were acquired every 15 s with an exposure time of 500 ms and 900 ms for the FlAsH and mCherry channels, respectively. DIC images were acquired at 15 s intervals with an exposure time of 1 s. Only those bacteria for which initial mammalian cell contact was observed were quantified. A total of 11 individual bacteria for the SptP-3XTC and 14 bacteria containing the SopE2-3XTC obtained from independent experiments on different days were used for analysis of type III secretion kinetics. The fluorescence intensity of individual bacteria was quantified by summing their intensity in an ROI (roughly the size of the bacterium) for both the FlAsH and reference mCherry channels. The fluorescence intensities for both channels were background subtracted, where an ROI of identical size was placed in a region of the dish containing no cells and no bacteria. Background-corrected FlAsH and mCherry signals were then processed as a ratiometric (FlAsH/mCherry) time course. Bleaching corrections were not performed on any data sets as independent experiments demonstrated that the rate of photobleaching was not significant compared to the rate of decay for our experimental conditions (see Figure 2). Kinetic traces were individually fit to single exponential equations, and the rate constant ($k_{secretion}$) and error in this fit were extracted. Only those bacteria that remained isolated for the majority of an experiment were included in the analysis. In the case of clear interference by other bacteria, as assessed by DIC and the mCherry channel, time course data points were excluded from exponential fits.

3,5-Dichlorosalicylaldehyde Benzoyl Hydrazone (1)

The type III secretion system inhibitor **1** was synthesized as described from commercially available starting materials (Sigma) (Johnson et al., 1982). Compound **1** was recrystallized from ethanol and confirmed to be >95% pure as assessed by NMR: ^{1}H NMR (600 MHz, D_6-DMSO) δ 12.54 (s, 2H), 8.58 (s, 1H) 7.96 (d, J = 7.8 Hz, 2H), 7.68 (d, J = 2.5 Hz, 1H), 7.63 (t, J = 7.3, 1H), 7.62 (d, J = 2.5 Hz, 1H), 7.56 (t, J = 7.8 Hz, 2H); ^{13}C NMR (600 MHz, D_6-DMSO) δ 163.07, 152.30, 147.10, 132.39, 132.20, 130.30, 128.67, 128.47, 127.81, 122.95, 121.49, 120.79. Inhibition of type III secretion was performed by pretreating invasion-induced *Salmonella* with 100 μM of compound **1** (DMSO as carrier) for 3 hr prior to the kinetic secretion assay. To enhance bacterial uptake with macrophage-like RAW264.7 infections, inhibitor-treated bacteria were opsonized with 14% fetal calf serum for 30 min prior to mammalian cell addition.

Proteasomal Degradation Assay

Host cell-mediated degradation rates of the effectors SopE2 and SptP were assessed using the method of Kubori and Galan (2003) with slight modifications. SL1344 strains carrying genomic 3XFLAG epitope fusions to the effector proteins SopE2 and SptP were grown under invasion conditions for ~16 hr at 37°C. HeLa cells (50%–80% confluence) were infected at an MOI of ~100 at 37°C and 5% CO_2. After 15 min of infection, cells were washed two times with warm HHBSS and overlaid with 10 ml of HHBSS containing 0.1 mg/ml of gentamycin (Sigma). For de novo protein synthesis inhibition experiments, 100 μg × ml^{-1} chloramphenicol was added to all time points 15 min postinvasion. Effector proteins were harvested at the appropriate time points by washing the cultures two times with cold HHBSS containing the proteasome inhibitor Mg132 (10 μM; Sigma) followed by lysis in 1.0 ml lysis buffer (HHBSS, 0.1% Triton X-100, 1 mM PMSF, and 10 μM Mg132). HeLa cell lysates were clarified by centrifugation at 14 krpm for 30 min (4°C). The supernatant fraction was filtered through a 0.2 μm filter, TCA precipitated, the proteins resolved by SDS-PAGE (10%–20% gradient), and transferred to PVDF membrane for western blotting. The membranes were simultaneously probed with a mouse anti-FLAG M2 antibody (1:500), mouse anti-β-actin antibody (1:7500), and rabbit antimouse HRP conjugate (1:5000) as secondary antibody. Membranes were stripped and reprobed with a mouse monoclonal anti-DnaK antibody (1:1000) to confirm the absence of bacterial cytoplasmic contaminants in the translocated effector fractions. SopE2 and SptP half-lives ($t_{1/2}$) were estimated by comparing the area times intensity, normalized to the β-actin loading control.

Statistical Analysis

All statistical tests were performed using GraphPad Prism software (GraphPad Software, Inc., La Jolla, CA). Statistical significance for FlAsH staining intensities was obtained using the Kruskal-Wallis test and Dunn's multiple comparison posttest. This nonparametric test was used because each group did not conform to normality as the mean fluorescence intensities were just above the detection limit of the system. For kinetic comparisons of the effectors SopE2- and SptP-3XTC, n values for secretion assays were obtained from individual experiments on separate days. A two-tailed unpaired t test was used for statistical analysis ($\alpha = 0.05$; $p = 0.0029$) and the assumption of equal variances was substantiated using an F test ($\alpha = 0.05$; $p = 0.4173$).

SUPPLEMENTAL DATA

Supplemental Data include seven figures, Supplemental Experimental Procedures, a Supplemental Reference, and one movie and can be found with this article online at http://www.chembiol.com/cgi/content/full/15/6/619/DC1/.

ACKNOWLEDGMENTS

We thank Corrella Detweiler for providing bacterial strains, plasmids, and advice; Richard Shoemaker for help with NMR samples and structure determination; and Jorge E. Galán for providing the monoclonal anti-SptP antibody. We acknowledge the Creative Training in Molecular Biology grant (NIH 5 T32 GM07135-33) and the University of Colorado for financial support. We declare no competing financial interests.

Received: November 13, 2007
Revised: April 15, 2008
Accepted: April 22, 2008
Published: June 20, 2008

REFERENCES

Abrahams, G.L., Muller, P., and Hensel, M. (2006). Functional dissection of SseF, a type III effector protein involved in positioning the *Salmonella*-containing vacuole. Traffic *7*, 950–965.

Adams, S.R., Campbell, R.E., Gross, L.A., Martin, B.R., Walkup, G.K., Yao, Y., Llopis, J., and Tsien, R.Y. (2002). New biarsenical ligands and tetracysteine

motifs for protein labeling in vitro and in vivo: synthesis and biological applications. J. Am. Chem. Soc. *124*, 6063–6076.

Akeda, Y., and Galan, J.E. (2005). Chaperone release and unfolding of substrates in type III secretion. Nature *437*, 911–915.

Collazo, C.M., and Galan, J.E. (1996). Requirement for exported proteins in secretion through the invasion-associated type III system of *Salmonella typhimurium*. Infect. Immun. *64*, 3524–3531.

Collazo, C.M., Zierler, M.K., and Galan, J.E. (1995). Functional analysis of the *Salmonella typhimurium* invasion genes invI and invJ and identification of a target of the protein secretion apparatus encoded in the inv locus. Mol. Microbiol. *15*, 25–38.

Datsenko, K.A., and Wanner, B.L. (2000). One-step inactivation of chromosomal genes in *Escherichia coli* K-12 using PCR products. Proc. Natl. Acad. Sci. U.S.A. *97*, 6640–6645.

Drecktrah, D., Knodler, L.A., Ireland, R., and Steele-Mortimer, O. (2006). The mechanism of *Salmonella* entry determines the vacuolar environment and intracellular gene expression. Traffic *7*, 39–51.

Enninga, J., Mounier, J., Sansonetti, P., and Tran, V.N. (2005). Secretion of type III effectors into host cells in real time. Nat. Methods *2*, 959–965.

Fu, Y., and Galan, J.E. (1999). A *Salmonella* protein antagonizes Rac-1 and Cdc42 to mediate host-cell recovery after bacterial invasion. Nature *401*, 293–297.

Hanahan, D. (1983). Studies on transformation of *Escherichia coli* with plasmids. J. Mol. Biol. *166*, 557–580.

Hapfelmeier, S., Ehrbar, K., Stecher, B., Barthel, M., Kremer, M., and Hardt, W.D. (2004). Role of the Salmonella pathogenicity island 1 effector proteins SipA, SopB, SopE, and SopE2 in *Salmonella enterica* subspecies 1 serovar Typhimurium colitis in streptomycin-pretreated mice. Infect. Immun. *72*, 795–809.

Hardt, W.D., Chen, L.M., Schuebel, K.E., Bustelo, X.R., and Galan, J.E. (1998). *S. typhimurium* encodes an activator of Rho GTPases that induces membrane ruffling and nuclear responses in host cells. Cell *93*, 815–826.

Huang, F.C., Werne, A., Li, Q., Galyov, E.E., Walker, W.A., and Cherayil, B.J. (2004). Cooperative interactions between Flagellin and SopE2 in the epithelial interleukin-8 response to *Salmonella enterica* Serovar Typhimurium infection. Infect. Immun. *72*, 5052–5062.

Hudson, D.L., Layton, A.N., Field, T.R., Bowen, A.J., Wolf-Watz, H., Elofsson, M., Stevens, M.P., and Galyov, E.E. (2007). Inhibition of *Salmonella* type III secretion by small-molecule inhibitors. Antimicrob. Agents Chemother. *51*, 2631–2635.

Johnson, D.K., Murphy, T.B., Rose, N.J., Goodwin, W.H., and Pickart, L. (1982). Cytotoxic chelators and chelates 1. Inhibition of DNA synthesis in cultured rodent and human cells by aroylhydrazones and by a copper(II) complex of salicylaldehyde benzoyl hydrazone. Inorganica Chimica. Acta *67*, 159–165.

Kubori, T., and Galan, J.E. (2003). Temporal regulation of *Salmonella* virulence effector function by proteasome-dependent protein degradation. Cell *115*, 333–342.

Martin, B.R., Giepmans, B.N., Adams, S.R., and Tsien, R.Y. (2005). Mammalian cell-based optimization of the biarsenical-binding tetracysteine motif for improved fluorescence and affinity. Nat. Biotechnol. *23*, 1308–1314.

Patel, J.C., Rossanese, O.W., and Galan, J.E. (2005). The functional interface between *Salmonella* and its host cell: opportunities for therapeutic intervention. Trends Pharmacol. Sci. *26*, 564–570.

Rudolph, M.G., Weise, C., Mirold, S., Hillenbrand, B., Bader, B., Wittinghofer, A., and Hardt, W.D. (1999). Biochemical analysis of SopE from *Salmonella typhimurium*, a highly efficient guanosine nucleotide exchange factor for RhoGTPases. J. Biol. Chem. *274*, 30501–30509.

Schlumberger, M.C., and Hardt, W.D. (2006). *Salmonella* type III secretion effectors: pulling the host cell's strings. Curr. Opin. Microbiol. *9*, 46–54.

Schlumberger, M.C., Muller, A.J., Ehrbar, K., Winnen, B., Duss, I., Stecher, B., and Hardt, W.D. (2005). Real-time imaging of type III secretion: *Salmonella* SipA injection into host cells. Proc. Natl. Acad. Sci. U.S.A. *102*, 12548–12553.

Shaner, N.C., Campbell, R.E., Steinbach, P.A., Giepmans, B.N., Palmer, A.E., and Tsien, R.Y. (2004). Improved monomeric red, orange and yellow fluorescent proteins derived from *Discosoma* sp. red fluorescent protein. Nat. Biotechnol. *22*, 1567–1572.

Sory, M.P., and Cornelis, G.R. (1994). Translocation of a hybrid YopE-adenylate cyclase from *Yersinia enterocolitica* into HeLa cells. Mol. Microbiol. *14*, 583–594.

Stender, S., Friebel, A., Linder, S., Rohde, M., Mirold, S., and Hardt, W.D. (2000). Identification of SopE2 from *Salmonella typhimurium*, a conserved guanine nucleotide exchange factor for Cdc42 of the host cell. Mol. Microbiol. *36*, 1206–1221.

Zhou, D., and Galan, J. (2001). *Salmonella* entry into host cells: the work in concert of type III secreted effector proteins. Microbes Infect. *3*, 1293–1298.

Zhou, D., Mooseker, M.S., and Galan, J.E. (1999). Role of the *S. typhimurium* actin-binding protein SipA in bacterial internalization. Science *283*, 2092–2095.

Zhou, D., Chen, L.M., Hernandez, L., Shears, S.B., and Galan, J.E. (2001). A *Salmonella* inositol polyphosphatase acts in conjunction with other bacterial effectors to promote host cell actin cytoskeleton rearrangements and bacterial internalization. Mol. Microbiol. *39*, 248–259.

